



CHORUS

This is the accepted manuscript made available via CHORUS. The article has been published as:

Pressure dependence of the exchange anisotropy in an organic ferromagnet

Komalavalli Thirunavukkuarasu, Stephen M. Winter, Christopher C. Beedle, Alexey E. Kovalev, Richard T. Oakley, and Stephen Hill

Phys. Rev. B **91**, 014412 — Published 12 January 2015

DOI: [10.1103/PhysRevB.91.014412](https://doi.org/10.1103/PhysRevB.91.014412)

Pressure Dependence of the Exchange Anisotropy in an Organic Ferromagnet

Komalavalli Thirunavukkuarasu,¹ Stephen M. Winter,² Christopher C. Beedle,¹ Alexey E. Kovalev,¹ Richard T. Oakley,^{2,*} and Stephen Hill^{1,†}

¹*National High Magnetic Field Laboratory and Department of Physics, Florida State University, Tallahassee, Florida 32310 USA*

²*Department of Chemistry, University of Waterloo, Waterloo, Ontario N2L 3G1 Canada*

The combination of high-pressure ferromagnetic resonance (FMR) and an ab-initio scheme suitable for calculation of spin-orbit mediated anisotropic exchange interactions in molecular materials provides insights into the role of spin-orbit coupling (SOC) in a Se-based organic ferromagnet. FMR measurements reveal a continuous increase in the magnetic anisotropy with increasing pressure (up to 2.2 GPa), in excellent agreement with calculations based on the known pressure-dependence of the structure. The large value of anisotropic exchange terms in this heavy atom organic ferromagnet emphasizes the important role of SOC in a wide range of organics where this effect is usually considered to be small.

I. INTRODUCTION

The discovery of weakly correlated materials with non-trivial band topologies has recently brought into prominence the study of spin-orbit coupling (SOC) in the solid state.^{1,2} This interaction also plays an important role in magnetic insulators, where SOC manifests itself as anisotropic exchange interactions between local spin-orbital moments.^{3,4} These anisotropic terms, such as the celebrated Dzyaloshinsky-Moriya interaction, are instrumental in many magnetic phenomena including magnetic coercivity and spin-canting, as well as the more exotic multiferroicity⁵ and topological spin phases.^{6–8} Engineering such states in real materials requires understanding the relationship between spin-orbit parameters and crystal structure, emphasizing the need for both experimental and ab-initio probes of SOC.⁹ In search of materials with strong SOC, the majority of developments in the field have focused on inorganic solids, drawing particularly from heavy elements with principle quantum number $n \geq 5$.^{10–13} In this report we focus instead on the bis-selenazoyl radical (Fig. 1(b), hereafter denoted **1**), a selenium-based organic ferromagnet in which significant SOC induced anisotropic exchange has been previously identified.^{14,15}

Compound **1** crystallizes in the non-centric tetragonal space group $P4_21m$, with each of the four molecules in the unit cell forming the basis for π -stacked radical “chains” extending in the c -direction (Fig. 1(a)).¹⁶ Each π -stack is bisected by a local mirror plane and neighbouring stacks are related by 2_1 axes. At ambient pressure, **1** is a Mott insulator, and orders as a bulk ferromagnet below $T_C = 17$ K. Previous ferromagnetic resonance (FMR) studies revealed uniaxial easy c -axis anisotropy characterized by a large anisotropy field $\mu_0 H_A = 0.88$ T at ambient pressure, which was shown to arise from anisotropic exchange between $S = \frac{1}{2}$ radical sites.^{14,15} It was shown that this degree of magnetic anisotropy is several orders of magnitude larger than one would expect on the basis of classical shape/demagnetizing effects,^{14,17} thus necessitating consideration of SOC mediated anisotropic

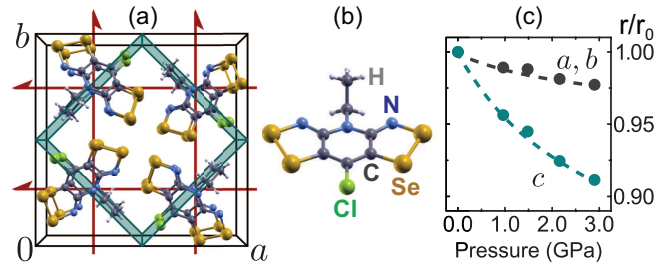


FIG. 1. (a) Crystallographic packing of radical **1** emphasizing π -stacking along the c -direction. Crystallographic mirror planes and 2_1 axes are shown. (b) Single radical molecule with atoms labelled. (c) Ratio of cell dimensions (r) to those at 0 GPa (r_0) as a function of pressure.

exchange interactions between $S = \frac{1}{2}$ radical sites (for which single site SOC anisotropy is forbidden in the absence of a magnetic field). Indeed, the observation of an anticipated reduction of H_A upon partial substitution of selenium ($n = 4$) for lighter sulfur ($n = 3$) has provided important indications of the importance of SOC physics,¹⁵ thereby motivating the present investigation of the pressure-dependence of inter-site hopping processes and their role in mediating anisotropic exchange interactions.

Under pressure, x-ray studies on **1** have demonstrated uniform compression of the unit cell, with approximately 2% and 7% reduction in a and c , respectively, up to 3 GPa (Fig. 1(c)).¹⁸ Concomitant with this compression is a reduction of the relative π -stack slippage, as measured by the angle between the normal of the molecular plane and crystallographic c -axis, which modulates the hopping integrals between adjacent radicals in the same π -stack. This effect initially enhances the isotropic ferromagnetic exchange, resulting in an increase of T_C from 17 K to 21 K at 1.0 GPa.^{18,19} At still higher pressures, further reduction of slippage finally drives the antiferromagnetic exchange within the stacks antiferromagnetic, and results in a monotonic decrease of T_C . In this report, we explore the evolution of SOC exchange terms through a recently developed high-pressure FMR technique. We also intro-

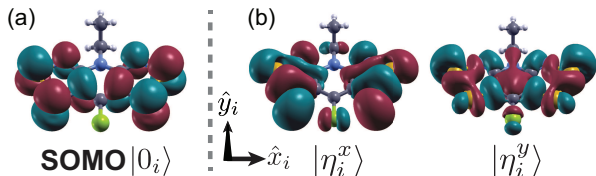


FIG. 2. (a) Highest occupied orbital (SOMO, $\alpha = 0$) at each radical site i . (b) pseudo-orbital functions defined in eq'n (6) to describe SOC hopping parameters \mathbf{C}_{00}^{ij} . The shape of $|\eta_i^\mu\rangle$ enhances anisotropic exchange between adjacent π -stacks.

duce an ab-initio scheme suitable for the calculation of these terms for organic materials. Using this scheme, we analyze various anisotropic exchange contributions to H_A .

II. AB-INITIO CALCULATIONS

In the following section, we describe a new scheme for accurate calculation of anisotropic exchange interactions for magnetic organic materials using quantum chemistry methods. At each radical site i , molecular orbitals are labeled by an index α_i , and have associated orbital energy ϵ_α . The highest occupied of these ($\alpha_i = 0$) is the π -antibonding singly occupied molecular orbital (SOMO) depicted in Fig. 2(a). Within the SOMO band, with inclusion of SOC effects, hopping is described by:

$$\mathcal{T} = \sum_{i,j} \mathbf{c}_{i,0}^\dagger \left(t_{00}^{ij} \mathbb{I} + \frac{1}{2} \sum_{\mu} [\mathbf{C}_{00}^{ij}]_{\mu} \sigma_{\mu} \right) \mathbf{c}_{j,0} + \text{H.c.} \quad (1)$$

where $\mu \in \{x, y, z\}$, σ_{μ} are Pauli matrices, and \mathbb{I} is the 2×2 identity matrix. The two component operator $\mathbf{c}_{i,0}^\dagger = (c_{i,0,\uparrow}^\dagger, c_{i,0,\downarrow}^\dagger)$ creates an electron in the SOMO at site i . Hopping integrals are denoted $t_{\alpha\alpha'}^{ij} = \langle \alpha_i | \mathcal{F} | \alpha_j' \rangle$, where \mathcal{F} is the Fock operator. The components of the purely imaginary spin-orbit hopping parameter \mathbf{C}_{00}^{ij} are given by a summation over all (valence) orbitals:

$$[\mathbf{C}_{00}^{ij}]_{\mu} = \sum_{\alpha \neq 0} \frac{\langle 0_i | \mathcal{L}_i^{\mu} | \alpha_i \rangle}{\epsilon_{\alpha} - \epsilon_0} t_{\alpha 0}^{ij} + t_{0\alpha}^{ij} \frac{\langle \alpha_j | \mathcal{L}_j^{\mu} | 0_j \rangle}{\epsilon_{\alpha} - \epsilon_0} \quad (2)$$

where \mathcal{L}_i^{μ} are effective orbital angular momentum operators for site i described in Ref. 20. Assuming a large and orbital independent Coulomb repulsion $U \gg \{t, \mathbf{C}\}$, perturbative treatment of the hopping gives rise to the spin Hamiltonian:

$$\mathcal{H} = \sum_{i,j} -\mathcal{J}_{ij} \mathbf{S}_i \cdot \mathbf{S}_j + \mathbf{D}_{ij} \cdot \mathbf{S}_i \times \mathbf{S}_j + \mathbf{S}_i \cdot \mathbf{\Gamma}_{ij} \cdot \mathbf{S}_j \quad (3)$$

where the cartesian components of the Dzyaloshinsky-Moriya (DM) vector \mathbf{D}_{ij} and pseudo-dipolar (PD) tensor

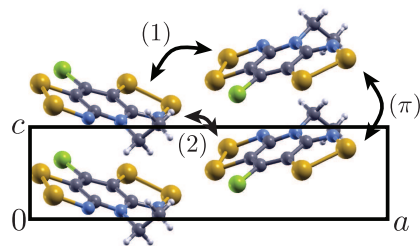


FIG. 3. Stacking of radicals **1** viewed parallel to the b -axis showing definition of interactions. (π)-type interactions occur between nearest neighbours in the same π -stack, while unique interstack interactions are labelled (1) and (2).

$\mathbf{\Gamma}_{ij}$ are given by:

$$[\mathbf{D}_{ij}]_{\mu} = \frac{2i}{U} \left([\mathbf{C}_{00}^{ij}]_{\mu} t_{00}^{ji} - t_{00}^{ij} [\mathbf{C}_{00}^{ji}]_{\mu} \right) \quad (4)$$

$$[\mathbf{\Gamma}_{ij}]_{\mu\nu} = \frac{1}{U} \left([\mathbf{C}_{00}^{ij}]_{\mu} [\mathbf{C}_{00}^{ji}]_{\nu} + [\mathbf{C}_{00}^{ji}]_{\mu} [\mathbf{C}_{00}^{ij}]_{\nu} \right) \quad (5)$$

In principle, \mathbf{D}_{ij} and $\mathbf{\Gamma}_{ij}$ may be estimated from zero-field splitting calculations in the triplet state of the radical pair (i, j) via wave function-based,²¹ or perturbative density functional-based approaches.²² However, given (i) the small magnitude of these terms ($\sim 0.1 - 1.0$ K), (ii) the importance of correlation effects, and especially (iii) the large number of potentially relevant valence orbitals $\{\alpha_i\}$ to consider in the SOC treatment, obtaining accurate estimates of \mathbf{D}_{ij} and $\mathbf{\Gamma}_{ij}$ for organics by existing methods represents a significant challenge. Our new approach instead uses density functional theory first to compute the hopping integrals (in the absence of SOC), orbital energies, and spin-orbit matrix elements, and then to compute \mathbf{C}_{00}^{ij} directly by eq'n (2). The anisotropic exchange parameters \mathbf{D}_{ij} and $\mathbf{\Gamma}_{ij}$ can then be estimated on the basis of Moriya's perturbative model (eq'ns (3) to (5)). Necessary terms for this calculation were computed using the ORCA package²³ on the basis of site-localized B3LYP/6-311G** orbitals, constructed to have maximum overlap with the corresponding orbitals in the isolated molecule. Orbital energies, ϵ_{α} , were approximated by the Kohn-Sham eigenvalues of the isolated molecules. Hopping integrals were estimated for each unique radical pair by rotation of the converged Fock matrix for the pair into the site local basis. Matrix elements of \mathcal{L}_i^{μ} were computed using the Spin Orbit Mean Field (SOMF) method implemented in the ORCA_soc module.^{20,24} Geometries for each radical pair were obtained from previously reported room temperature structures in the range 0.0–3.0 GPa.¹⁸ The Coulomb repulsion, $U \sim 0.8$ eV, was experimentally estimated from solution electrochemical measurements on **1** and related S/Se variants.¹⁶

In the solid state, compound **1** has three unique nearest neighbour pairs (i, j), as shown in Fig. 3. The first of these, for which i and j are in the same π -stack and related by translation along the c -axis, is labelled (π). The

remaining two, in which i and j are in different π -stacks and related by 2_1 axes at $c = \frac{1}{2}$ and 0, are labelled (1) and (2), respectively. Results of calculations are summarized in Fig. 4, with numerical values given in the supplemental information. The small scatter in the computed values may be related to uncertainty in the high pressure structural parameters, which were obtained by rigid body refinement of powder diffraction data rather than single crystal methods. At ambient pressure, we find that the largest SOMO-SOMO hopping integral t_{00}^{ij} occurs for (π) -type interactions, between adjacent radicals within the same π -stack. In contrast, the spin-orbit mediated hopping parameters $|\mathbf{C}_{00}^{ij}|$ are greatest between π -stacks. For all three interactions, the largest component of \mathbf{C}_{00}^{ij} lies within the crystallographic ab -plane. In order to facilitate qualitative discussion of these results, it is useful to interpret the orbital summation of eq'n (2) as defining a set of orbital-like functions $|\eta_i^\mu\rangle$ shown in Fig. 2(b):

$$|\eta_i^\mu\rangle = \sum_{\alpha \neq 0} |\alpha_i\rangle \frac{\langle \alpha_i | \mathcal{L}_i^\mu | 0_i \rangle}{\epsilon_\alpha - \epsilon_0} \quad (6)$$

The purely imaginary $|\eta_i^\mu\rangle$ functions are neither normalized nor eigenstates of the Fock operator, and so have no well-defined ϵ , but consideration of their spatial density and symmetry properties is nonetheless useful. In terms of these functions the components of the spin-orbit mediated hopping parameter \mathbf{C}_{00}^{ij} are simply hopping integrals between the SOMO and $|\eta_i^\mu\rangle$ functions on adjacent radicals:

$$\left[\mathbf{C}_{00}^{ij} \right]_\mu = t_{\eta^\mu 0}^{ij} + t_{0\eta^\mu}^{ij} \quad (7)$$

The magnitude and character of the anisotropic exchange between any two radicals may therefore be anticipated from the shapes of the $|\eta_i^\mu\rangle$ functions. For the purpose of discussion, we define local coordinates for each molecular site i , shown in Fig. 2: the \hat{x}_i -axis is normal to the crystallographic mirror plane bisecting the molecule, while the \hat{z}_i -axis is oriented along the normal of the molecular plane. For this choice of coordinates, the π -SOMO is approximately a linear combination of p_z orbitals, so that $|\eta_i^z\rangle \sim 0$ since $\mathcal{L}_i^z |0_i\rangle \sim 0$. This result, which is easily confirmed by ab-initio calculation, holds for any planar organic π -system and suggests that \mathbf{C}_{00}^{ij} will tend to be oriented perpendicular to \hat{z}_i and \hat{z}_j , since $t_{\eta^z 0}^{ij}$ vanishes. For radical **1** this preference ensures that all \mathbf{C}_{00}^{ij} lie within, or close to the crystallographic ab -plane. The remaining functions $|\eta_i^x\rangle$ and $|\eta_i^y\rangle$ are linear combinations of orbitals in the σ -framework, and have density largely confined within the molecular plane, but with significant extension around the periphery of the molecule. This shape enhances *interstack* $t_{\eta^\mu 0}^{ij}$ integrals which explains the finding that $|\mathbf{C}_{00}^{ij(1)}|, |\mathbf{C}_{00}^{ij(2)}| > |\mathbf{C}_{00}^{ij(\pi)}|$.

Under pressure, we find that $t_{00}^{ij(1)}$ remains relatively constant while $|t_{00}^{ij(\pi)}|$ and $|t_{00}^{ij(2)}|$ are initially suppressed

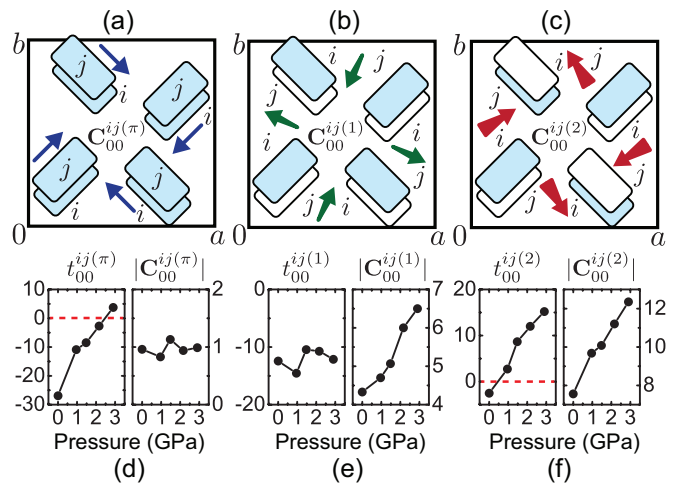


FIG. 4. (a)-(c): Orientations of the local \mathbf{C}_{00}^{ij} , viewed down the c -axis for interactions (π) , (1) , and (2) , respectively. Molecules are represented by boxes, with shaded boxes indicating interacting molecules (see Fig. 3). For interactions (1) and (2) , \mathbf{C}_{00}^{ij} has components in the c -direction, as indicated by tapered arrows. (d)-(f): Calculated t_{00}^{ij} and $|\mathbf{C}_{00}^{ij}|$ in meV as a function of pressure. The orientation of $|\mathbf{C}_{00}^{ij}|$ is relatively constant with pressure.

as both hopping integrals are driven more positive (from initially negative ambient pressure values). This effect, which was previously anticipated in Ref. 18, results in a reduction of antiferromagnetic exchange $\mathcal{J}_{AFM} \sim 4(t_{00}^{ij})^2/U$, and thus explains the enhancement of the ferromagnetic ordering T_C up to 1.0 GPa. In contrast, $|\mathbf{C}_{00}^{ij(1)}|$ and $|\mathbf{C}_{00}^{ij(2)}|$ are predicted to increase monotonically (Fig. 4) with pressure, while $|\mathbf{C}_{00}^{ij(\pi)}|$ remains small. This observation implies important consequences for the pressure dependence of the anisotropic exchange parameters \mathbf{D}_{ij} and $\mathbf{\Gamma}_{ij}$, which we have estimated from the computed \mathbf{C}_{00}^{ij} and t_{00}^{ij} values (see supplemental). From eq'n (4), it is easy to see that $\mathbf{D}_{ij} \parallel \mathbf{C}_{00}^{ij}$, so that the DM-interaction is minimized when the spins at sites (i, j) are canted, and lie in the plane $\mathbf{S}_i, \mathbf{S}_j \perp \mathbf{C}_{00}^{ij}$. For ferromagnetically oriented spins, the pseudo-dipolar interaction is also minimized for this orientation, which may be seen by rotating $\mathbf{\Gamma}_{ij}$ so that one of the principle axes is parallel to \mathbf{C}_{00}^{ij} . In this case, for example:

$$\mathbf{\Gamma}_{ij} = \frac{2}{U} \begin{pmatrix} 0 & 0 & 0 \\ 0 & 0 & 0 \\ 0 & 0 & +|\mathbf{C}_{00}^{ij}|^2 \end{pmatrix} \quad (8)$$

which is minimized, for parallel spins, when $\langle \mathbf{S}_i \cdot \mathbf{\Gamma}_{ij} \cdot \mathbf{S}_j \rangle = 0$, for $\mathbf{S}_i, \mathbf{S}_j \perp \mathbf{C}_{00}^{ij}$. As a result \mathbf{D}_{ij} and $\mathbf{\Gamma}_{ij}$ provide complementary contributions to the magnetocrystalline anisotropy. However, the small values of t_{00}^{ij} required for net ferromagnetic interactions also result in small \mathbf{D}_{ij} in **1**, so that $\mathbf{\Gamma}_{ij}$ represents the most important contribution to the anisotropy. To a first approximation, we therefore ignore contributions from the DM-interaction,

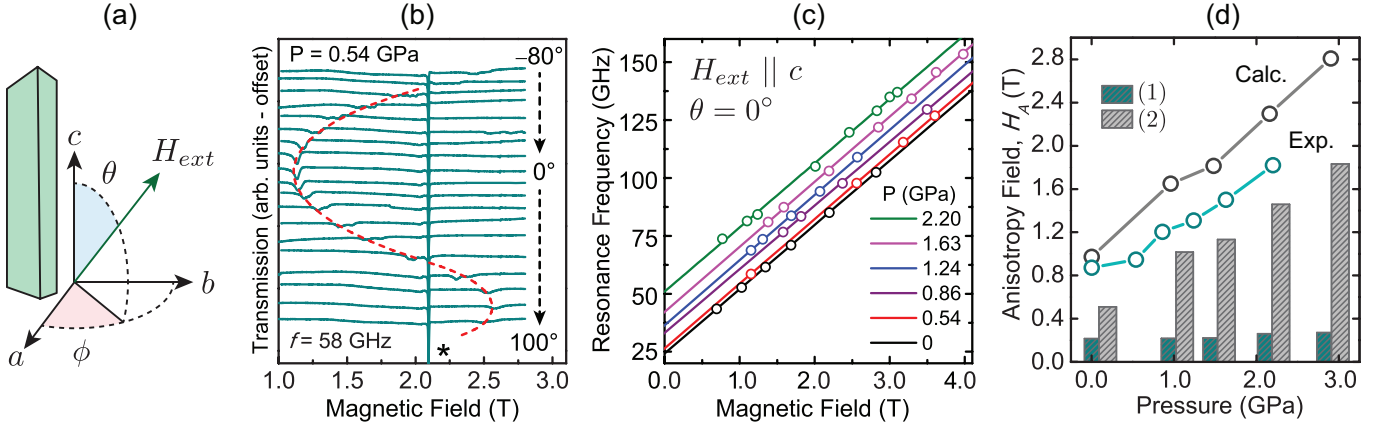


FIG. 5. (a) Schematic of the sample and experimental coordinates. (b) Angle dependent FMR spectra recorded as a function of the polar angle θ at $f = 58$ GHz and $T = 2$ K. The angle-dependent dip in transmission (red dash line is a guide to the eye) corresponds to FMR, while the sharp resonance marked by an asterisk (*) corresponds to an impurity signal (see main text). (c) Field dependence of f_{res} as a function of pressure for $\theta = 0^\circ$. (d) Comparison of experimental (for $T = 2$ K) and calculated values of H_A as a function of pressure, with contributions from interactions (1) and (2) indicated by the heights of the bars. The contribution from (π) interactions is negligible on this scale.

and assume a collinear magnetic structure. The finding that \mathbf{C}_{00}^{ij} tends to be oriented close to the ab -plane for all pairs of radicals is thus consistent with the observed easy c -axis anisotropy, which is associated with a zero-field gap Δ_{zf} in the collective ferromagnon spectrum at $k = 0$ (see Refs. 14 and 15 for a detailed explanation):

$$\Delta_{zf} \equiv g\mu_o\mu_B H_A = \frac{1}{2} \sum_j [\Gamma_{ij}]_{aa} + [\Gamma_{ij}]_{bb} - 2[\Gamma_{ij}]_{cc} \quad (9)$$

where the summation is over nearest neighbours, $\{a, b, c\}$ refer to the crystallographic axes, and H_A is the so-called anisotropy field. Calculated values of H_A as a function of pressure are shown in Fig. 5(d).

III. FMR MEASUREMENTS

In order to probe correlations between H_A and the crystal structure and, hence, obtain experimental insights into the SOC in **1**, we employed recently developed instrumentation capable of performing multi-high-frequency EPR (in this case, FMR) measurements under quasi-hydrostatic pressure. Below T_C , resonant absorption of microwave radiation occurs whenever the excitation energy of the $k = 0$ ferromagnon can be tuned by an external field to match the microwave frequency.^{25,26} For this reason, FMR is uniquely sensitive to the anisotropic components of the Hamiltonian. Combining FMR with high pressure techniques is challenging and unexplored. In this work, high-pressures were obtained using a plastic diamond anvil cell (DAC).²⁷ Multi-frequency, high pressure FMR measurements were then performed using a cavity perturbation technique (described in Refs 28 and

29) by placing the pressure cell inside a cylindrical resonator (a cavity) with dimensions matched to those of the DAC.^{30,31} Introduction of the plastic cell significantly increases the microwave losses within the resonator, thus suppressing its quality factor, making the measurements considerably more challenging than those at ambient pressure. Nevertheless, the losses can be minimized by working at low temperatures (< 10 K), enabling FMR measurements up to 2.2 GPa in the $f = 40 - 160$ GHz frequency range on small single-crystals of **1** (dimensions $0.1 \times 0.1 \times 0.2$ mm³). At each pressure, alignment of the sample with respect to the applied field was achieved by performing two-axis crystal rotation studies using a vector magnet (see Fig. 5(a) for a schematic showing the crystal and experimental coordinates). The pressure in the DAC was mediated using a 1:1 mixture of Fluorinert 70:77, and calibrated *in situ* at the measurement temperature by recording the luminescence from a ruby chip via the diamond window and an optical fiber.³² FMR spectra recorded at different polar angles, θ (ϕ undetermined), are shown in Fig. 5(b). The FMR signal is seen as a dip in the transmission through the cavity; its obvious angle-dependence distinguishes it from a strong angle-independent $g = 2$ impurity signal from the diamonds in the DAC. At high fields, the FMR position, H_{res} , for **1** was found to vary as:

$$H_{res} \approx \frac{hf_{res}}{g\mu_o\mu_B} - \frac{H_A}{2} (3 \cos^2 \theta - 1) \quad (10)$$

in accordance with the expected resonance condition for the easy c -axis anisotropy.^{14,15} The minimum of the resonance field yields the orientation of the easy c -axis ($\theta = 0^\circ$). For this orientation, the resonance frequency follows the relation:

$$hf_{res} = g\mu_o\mu_B (H_{res} + H_A) \quad (11)$$

allowing H_A to be extracted from multifrequency measurements (Fig. 5(c)).

IV. DISCUSSION

The sensitivity of the anisotropic exchange in **1** to structural details is highlighted by the near doubling of H_A over the range 0.0 – 2.2 GPa, despite relatively small contraction of the unit cell (i.e. 2% for the a, b axes and 7% for the c -axis). Close agreement is found between experimental H_A values and those calculated from eq'n (9) in terms of both sign and magnitude. At ambient pressure, for example, the calculated value of 0.97 T compares favorably with the experimental value of $\mu_0 H_A = 0.88$ T (Fig. 5(d)). The monotonic increase of H_A found experimentally under pressure is also correctly reproduced. As explained above, this enhancement of H_A under pressure can be attributed to an average increase of $t_{0\eta^\mu}^{ij}$ integrals for *interstack* interactions, which by eq'n (7) leads to a uniform enhancement of \mathbf{C}_{00}^{ij} and thus $\mathbf{\Gamma}_{ij}$. This enhancement can be visually anticipated from the shapes of the $|\eta_i^\mu\rangle$ functions, which have simple lobal structures around the molecular periphery, allowing the weighted hopping integrals $t_{0\eta^\mu}^{ij}$ to increase uniformly with compression for interactions (1) and (2). In contrast, the lobal mismatch between the SOMO $|0_i\rangle$ and $|\eta_j^\mu\rangle$ on adjacent molecules in the same π -stack results in a small and pressure independent \mathbf{C}_{00}^{ij} associated with nearly isotropic *intrastack* interactions at all pressures. Interestingly, the calculations also suggest that H_A arises almost entirely from *interstack* interactions (1) and (2), with (π) interactions contributing less than 2% of the observed H_A , in contrast with our previous assumptions.¹⁵ The finding that the pressure dependence of t_{00}^{ij} and \mathbf{C}_{00}^{ij} (and thus the isotropic and anisotropic interactions) is largely unrelated also has implications for studies of other spin-orbit coupled materials under pressure.^{33,34}

Taken together, the close agreement between the experimental and theoretical H_A values over the studied pressure range validates the magnitude of the calculated spin-orbit hopping parameters $|\mathbf{C}_{00}^{ij}| \sim 10$ meV, which, in the present material, are of similar magnitude to the hopping parameters $t_{00}^{ij} \sim 10$ meV. However, for organic materials in general, typically $t \lesssim 100$ meV,³⁵ suggesting for Se-based organics that $|\mathbf{C}|/t \sim 10\%$ represents a reasonable estimate, and such materials should therefore be considered moderate to strongly spin-orbit coupled. This suggestion follows from a key feature of organics: due to their molecular nature, all relevant energy scales, such as hopping integrals t , Coulomb repulsion U , and orbital

energy splittings $\Delta\epsilon$, are often at least an order of magnitude smaller than for inorganic materials. Thus SOC, the scale of which is set in molecular systems by the heaviest constituent atoms, may play a significant role for the organics despite their being composed of relatively lighter elements than their $n \geq 5$ inorganic counterparts.

Although light heteroatom ($n = 2, 3$) organic magnetic materials have a long history, heavy atom ($n > 3$) radical magnets have emerged only recently; they simply were not known before 2006 because of the strong tendency for the radicals to dimerize and form non-magnetic singlet ground states. Continued research into such systems may well provide a rich source of new SOC related physics. For example, the possibility of realizing topologically nontrivial phases in organics remains essentially unexplored.³⁶ Although weaker than in their selenium-based counterparts, anisotropic exchange terms have also been implicated in magnetically ordered sulfur-based organics, such as the spin-canted antiferromagnets (BEDT-TTF)₂Cu[N(CN)₂]Cl,^{37–39} *p*-NC-C₆F₄-CNSSN,⁴⁰ and FBBO.⁴¹ A comprehensive study of the SOC effects in these and other organic materials is of great interest and importance.

In summary, we have introduced an ab-initio scheme suitable for calculation of spin-orbit hopping parameters, \mathbf{C}_{00}^{ij} , in organic materials. Combining this method with high pressure FMR measurements has allowed investigation of the structural aspects of SOC in the Se-based ferromagnet **1**. With increasing pressure, the anisotropy field measured by FMR increases continuously, consistent with the theoretical calculations that predict strong enhancement of interstack anisotropic exchange with pressure. The large relative magnitude of the SOC terms suggests significant modification of both the magnetic and electronic excitations in this heavy atom ferromagnet, prompting reconsideration of the role of SOC in a broad range of other organics.

V. ACKNOWLEDGEMENTS

We thank the NSERC (Canada) and the US NSF (Grant Nos. DMR-1309463 and CHE-0924374) for financial support. S.M.W. acknowledges NSERC for a Graduate Scholarship. K.T. acknowledges support via Feodor-Lynen fellowship from Alexander von Humboldt foundation (Germany). The NHMFL is supported by the NSF (DMR-1157490) and by the State of Florida. Finally, we thank Dr. Stanley W. Tozer for his support in the development of high pressure EPR technique.

* oakley@uwaterloo.ca

† shill@magnet.fsu.edu

¹ M. Z. Hasan and C. L. Kane, Rev. Mod. Phys. **82**, 3045 (2010).

- ² B. A. Bernevig and T. L. Hughes, *Topological Insulators and Topological Superconductors* (Princeton University Press, 2013).
- ³ T. Moriya, Phys. Rev. **120**, 91 (1960).
- ⁴ I. Dzyaloshinsky, Journal of Physics and Chemistry of Solids **4**, 241 (1958).
- ⁵ K. F. Wang, J.-M. Liu, and Z. F. Ren, Advances in Physics **58**, 321 (2009).
- ⁶ D. Hsieh, Y. Xia, L. Wray, D. Qian, A. Pal, J. H. Dil, J. Osterwalder, F. Meier, G. Bihlmayer, C. L. Kane, Y. S. Hor, R. J. Cava, and M. Z. Hasan, Science **323**, 919 (2009).
- ⁷ S. Muhlbauer, B. Binz, F. Jonietz, C. Pfleiderer, A. Rosch, A. Neubauer, R. Georgii, and P. Boni, Science **323**, 915 (2009).
- ⁸ J. Zaanen, Science **323**, 888 (2009).
- ⁹ V. E. Dmitrienko, E. N. Ovchinnikova, S. P. Collins, G. Nisbet, G. Beutier, Y. O. Kvashnin, V. V. Mazurenko, A. I. Lichtenstein, and M. I. Katsnelson, Nature Physics **10**, 202 (2014).
- ¹⁰ D. Pesin and L. Balents, Nature Physics **6**, 376 (2010).
- ¹¹ W. Witczak-Krempa, G. Chen, Y. B. Kim, and L. Balents, Annual Review of Condensed Matter Physics **5**, 57 (2014).
- ¹² P. Dziawa, Nat Mater **11**, 1023 (2012).
- ¹³ S. Chadov, X. Qi, J. Kübler, G. H. Fecher, C. Felser, and S. C. Zhang, Nat Mater **9**, 541 (2010).
- ¹⁴ S. M. Winter, S. Datta, S. Hill, and R. T. Oakley, J. Am. Chem. Soc. **133**, 8126 (2011).
- ¹⁵ S. M. Winter, R. T. Oakley, A. E. Kovalev, and S. Hill, Phys. Rev. B **85**, 094430 (2012).
- ¹⁶ C. M. Robertson, A. A. Leitch, K. Cvrkalj, R. W. Reed, D. J. T. Myles, P. A. Dube, and R. T. Oakley, J. Am. Chem. Soc. **130**, 8414 (2008).
- ¹⁷ J.-L. Stanger, J.-J. André, P. Turek, Y. Hosokoshi, M. Tamura, M. Kinoshita, P. Rey, J. Cirujeda, and J. Veciana, Phys. Rev. B **55**, 8398 (1997).
- ¹⁸ M. Mito, Y. Komorida, H. Tsuruda, J. S. Tse, S. Desgreniers, Y. Ohishi, A. A. Leitch, K. Cvrkalj, C. M. Robertson, and R. T. Oakley, J. Am. Chem. Soc. **131**, 16012 (2009).
- ¹⁹ H. Tsuruda, M. Mito, H. Deguchi, S. Takagi, A. A. Leitch, K. Lekin, S. M. Winter, and R. T. Oakley, Polyhedron **30**, 2997 (2011).
- ²⁰ F. Neese, J. Chem. Phys. **122**, 034107 (2005).
- ²¹ D. Ganyushin and F. Neese, J. Chem. Phys. **125**, 024103 (2006).
- ²² F. Neese, J. Chem. Phys. **127**, 164112 (2007).
- ²³ F. Neese, Wiley Interdisciplinary Reviews: Computational Molecular Science **2**, 73 (2012).
- ²⁴ B. A. Hess, C. M. Marian, U. Wahlgren, and O. Gropen, Chemical Physics Letters **251**, 365 (1996).
- ²⁵ A. G. Gurevich and G. A. Melkov, *Magnetization Oscillations and Waves* (Taylor & Francis, 1996).
- ²⁶ S. Vonsovskii, *Ferromagnetic resonance* (Pergamon Press, 1968).
- ²⁷ D. E. Graf, R. L. Stillwell, K. M. Purcell, and S. W. Tozer, High Pressure Research **31**, 533 (2011).
- ²⁸ M. Mola, S. Hill, P. Goy, and M. Gross, Rev. Sci. Instrum. **71**, 186 (2000).
- ²⁹ S. Takahashi and S. Hill, Rev. Sci. Instrum. **76**, 023114 (2005).
- ³⁰ A. Prescimone, C. Morien, D. Allan, J. A. Schlueter, S. W. Tozer, J. L. Manson, S. Parsons, E. K. Brechin, and S. Hill, Angew. Chem. Int. Ed. **51**, 1 (2012).
- ³¹ C. Beedle, S. Hill, and S. W. Tozer, to be published (2014).
- ³² J. D. Barnett, S. Block, and G. J. Piermarini, Rev. Sci. Instrum. **44**, 1 (1973).
- ³³ J. Zhu, J. L. Zhang, P. P. Kong, S. J. Zhang, X. H. Yu, J. L. Zhu, Q. Q. Liu, X. Li, R. C. Yu, R. Ahuja, W. G. Yang, G. Y. Shen, H. K. Mao, H. M. Weng, X. Dai, Z. Fang, Y. S. Zhao, and C. Q. Jin, Sci. Rep. **3** (2012).
- ³⁴ B. J. Yang, R. Arita, N. Nagaosa, and M. S. Bahramy, Nat Comms **3**, 679 (2012).
- ³⁵ N. Toyota, M. Lang, and J. Müller, *Low-Dimensional Molecular Metals*, Springer Series in Solid-State Sciences (Springer, 2007).
- ³⁶ Z. F. Wang, Z. Liu, and F. Liu, Nat Comms **4**, 1471 (2013).
- ³⁷ D. F. Smith, S. M. De Soto, C. P. Slichter, J. A. Schlueter, A. M. Kini, and R. G. Daugherty, Phys. Rev. B **68**, 024512 (2003).
- ³⁸ D. F. Smith, C. P. Slichter, J. A. Schlueter, A. M. Kini, and R. G. Daugherty, Phys. Rev. Lett. **93**, 167002 (2004).
- ³⁹ P. Lunkenheimer, J. Müller, S. Krohns, F. Schrettle, A. Loidl, B. Hartmann, R. Rommel, M. de Souza, C. Hotta, J. A. Schlueter, and M. Lang, Nat Mater **11**, 755 (2012).
- ⁴⁰ F. Palacio, G. Antorrena, M. Castro, R. Burriel, J. Rawson, J. N. B. Smith, N. Bricklebank, J. Novoa, and C. Ritter, Phys. Rev. Lett. **79**, 2336 (1997).
- ⁴¹ S. M. Winter, A. Mailman, R. T. Oakley, K. Thirunavukkuarasu, S. Hill, D. E. Graf, S. W. Tozer, J. S. Tse, M. Mito, and H. Yamaguchi, Phys. Rev. B **89**, 214403 (2014).